

## Final Report

**DOE Award Number:** DE-SC0005062

**Project Title:** Development of Ultrafiltration Membrane-Separation Technology for Energy-Efficient Water Treatment and Desalination Process

**Principal Investigator:** Woosoon Yim, Ph.D.

University of Nevada Las Vegas  
4505 Maryland Parkway, Box 454003  
Las Vegas, Nevada 89154-4003

**Co-Principal Investigator:** Chulsung Bae, Rensselaer Polytechnic Institute

**Reporting Period:** September 15, 2010 to September 14, 2016

### Table of Contents

<u>Contents</u>	<u>Page</u>
1. Background	2
2. Accomplishments	3
3. Comparison of accomplishment and explanation of variance	17
4. Plans for next report period	17
5. Cost status	17
6. Schedule status	17
7. Changes in approach or aims and reasons	17
8. Actual or anticipated problems or delays	17
9. Changes of key personnel	17
10. Product produced or technology transfer activities	17

## 1. Background

The growing scarcity of fresh water is a major political and economic challenge in the 21<sup>st</sup> century. Compared to thermal-based distillation technique of water production, pressure driven membrane-based water purification process, such as ultrafiltration (UF), nanofiltration (NF) and reverse osmosis (RO), can offer more energy-efficient and environmentally friendly solution to clean water production. Potential applications also include removal of hazardous chemicals (i.e., arsenic, pesticides, organics) from water. Although those membrane-separation technologies have been used to produce drinking water from seawater (desalination) and non-traditional water (i.e., municipal wastewater and brackish groundwater) over the last decades, they still have problems in order to be applied in large-scale operations. Currently, a major huddle of membrane-based water purification technology for large-scale commercialization is membrane fouling and its resulting increases in pressure and energy cost of filtration process. Membrane cleaning methods, which can restore the membrane properties to some degree, usually cause irreversible damage to the membranes. Considering that electricity for creating of pressure constitutes a majority of cost (~50%) in membrane-based water purification process, the development of new nano-porous membranes that are more resistant to degradation and less subject to fouling is highly desired.

Styrene-ethylene/butylene-styrene (SEBS) block copolymer (Figure 1) is one of the best known block copolymers that induces well defined morphologies. Due to the polarity difference of aromatic styrene unit and saturated ethylene/butylene unit (derived from polymerization of 1,3-butadiene followed by hydrogenation), these two polymer chains self-assemble each other and form different phase-separated morphologies depending on the ratios of two polymer chain lengths. Because the surface of SEBS is hydrophobic which easily causes fouling of membrane, incorporation of ionic group (e,g, sulfonate) to the polymer is necessary to reduces fouling. Recently, sulfonated SEBS became commercially available and has been extensively explored for membrane-mediated water purification technology. The sulfonated block copolymer creates a well developed nano-scale phase-separated morphologies composed of hydrophilic domains (sulfonated polystyrene) and hydrophobic domains (polyethylene/polybutylene). The hydrophilic domains determines transport properties (water transport, salt and/or ion rejection, etc) and the hydrophobic domains provides mechanical stability of the membrane. Unfortunately, a high degree of sulfonation of SEBS induces excessive swelling and deterioration of mechanical stability of the membrane.

In an effort to develop robust polymeric membrane materials for water purification technology, phosphonic acid-functionalized SEBS membranes are investigated during this report period. In compare to sulfonated polymers, the corresponding phosphonated polymers are known to swell less because of the formation of extensive hydrogen bonding networks between phosphonates. In addition to the expected better mechanical stability, phosphonated polymers has another advantage over sulfonated polymers for the use water purification membrane; each phosphonate can accommodate two ions while each sulfonate accommodates only one ion. Membrane properties (ion type, ionic density, etc) of new membranes will be studied and their separation performance will be evaluated in water purification and desalination process. Through systematic study of the relationship of chemical structure–surface property–membrane performance, we aim to better understand the nature of membrane fouling and develop more fouling-resistant water purification membranes. The basic understanding of this relationship will lead to the development of advanced membrane materials which can offer a solution to environmentally sustainable production of fresh water.

## 2. Accomplishments

### Characterization of SEBS ionomers

Once different ionic groups were incorporated to SEBS polymer, their membrane properties were investigated. Figure 1 shows the chemical structures of the ionic polymers: fluoroalkylsulfoanted SEBS-S<sub>1</sub>, arylsulfoanted SEBS-S<sub>2</sub>, phosphonated SEBS-P<sub>1</sub>. Ion exchange capacity (IEC), which is defined as the ratio between the number of acid groups (in mmol or mequiv) and the weight of dry membrane in gram, was measured using a titration method. Successful conversion of sulfonate or phosphonate ester to the corresponding acids can be confirmed quantitatively by comparing experimentally measured IEC (IEC<sub>Exp</sub>) with theoretical IEC (IEC<sub>Theo</sub>) which was calculated from <sup>1</sup>H NMR data (i.e., 18 mol% functionalization). As listed in Table 1, the IEC<sub>Exp</sub> values of SEBS-S<sub>1a</sub> and SEBS-S<sub>2a</sub> matched well with their IEC<sub>Theo</sub> whereas for SEBS-P<sub>1a</sub> the IEC<sub>Exp</sub> is slightly lower than the IEC<sub>Theo</sub>. This trend is commonly observed for phosphonic acid containing polymers because the second proton of the phosphonic acid is less acidic and may not be completely neutralized by hydroxide solution. Additionally, the sample drying step can lead to the formation of a mixture of free phosphonic acids and anhydrides in the polymer film.

Water uptake is an important parameter that influences mechanical properties and proton conductivity in both sulfonated and phosphonated membranes. In sulfonated polymers, the IEC values of the membranes generally dominate the water uptake of the membranes, and high water uptake leads to efficient water assisted proton transportation. In contrast, the high degree of hydrogen bonding and the lower acidity of the phosphonic acid groups can limit the water uptake behaviour of the membranes in the phosphonated polymers. SEBS-P<sub>1a</sub> showed a water uptake of only 0.4% while SEBS-S<sub>2a</sub> showed as high as 32%.

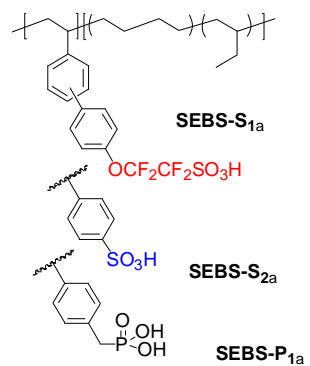


**Figure 1.** Structures of SEBS ionomers functionalized with different acid groups: SEBS-S<sub>1a</sub>, SEBS-S<sub>2a</sub>, and SEBS-P<sub>1a</sub>.

**Table 1** Membrane properties of acid-functionalized SEBS and Nafion.

SEBS Ionomer	Water Uptake (60 °C)	IEC (mequiv/g)		$\sigma$ (mS/cm) <sup>c</sup>
		Exp. <sup>a</sup>	Cal. <sup>b</sup>	
SEBS-S <sub>1a</sub>	22	1.55	1.58	43
SEBS-S <sub>2a</sub>	32	1.94	1.94	73
SEBS-P <sub>1a</sub>	4	3.56	3.78	0.4
Nafion 112	26	0.92	0.90	56

<sup>a</sup> Measured from titration method; <sup>b</sup> Estimated values from <sup>1</sup>H NMR spectra of protected sulfonated/phosphonated SEBS; <sup>c</sup> Proton conductivity measured at 60 °C and 100% relative humidity.

Thermal stability of ion-functionalized polymer samples was studied with TGA under a nitrogen atmosphere at a heating rate of 10 °C/min (Figure 2). While the decomposition temperature of pristine SEBS was recorded as 447 °C, the TGA curve of SEBS-S<sub>2a</sub> was characterized by three distinct regions of mass loss: (i) loss of water molecules bound to the

sulfonic acid of the membrane (at 50 to  $\sim$ 200 °C), (ii) elimination of sulfonic acid (around 260 °C), and (iii) degradation of polymer backbone (around 450 °C).

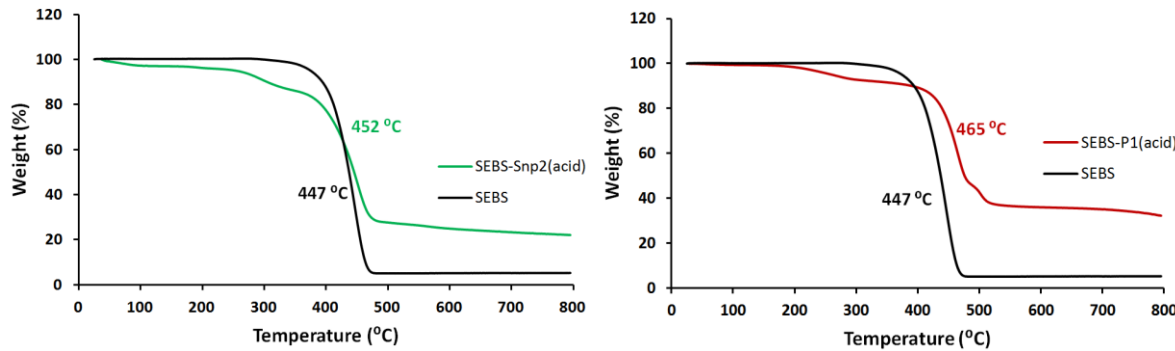


**Figure 2.** TGA data of SEBS, SEBS-S<sub>2a</sub>, and SEBS-P<sub>1a</sub>

A comparison of thermal behaviour of the phosphonated polymer and pristine SEBS is also shown in Figure 2. The initial minor weight loss (5–10%) between 170–300 °C is attributed to the formation of anhydrides by creation of P—O—P anhydride linkages. These anhydrides may be formed intermolecularly or intramolecularly. These bonds can be hydrolyzed to form phosphonic acid group when membranes are hydrated. The second weight loss was observed at 465 °C, which is attributed to the degradation of the polymer backbone.

Proton conductivity of a PEM is considered to be one of the most significant properties in fuel cell performance because the membrane conductivity is directly related to the power density. In four consecutive runs of proton conductivity measurements, the identical membrane sample of SEBS-S<sub>2a</sub> maintained a consistent value of proton conductivity at 60 °C and 100% RH implying that this membrane is stable under the measurement condition. Proton conductivity is heavily dependent upon the hydration level of conducting membrane when the Vehicular mechanism dominantly contributes to the proton conduction. Although SEBS-S<sub>2a</sub> membrane exhibited higher proton conductivity than Nafion 112 at RH above 80%, it's conductivity values dropped sharply at lower RH, which is common for most hydrocarbon-based PEM materials (Figure 3).

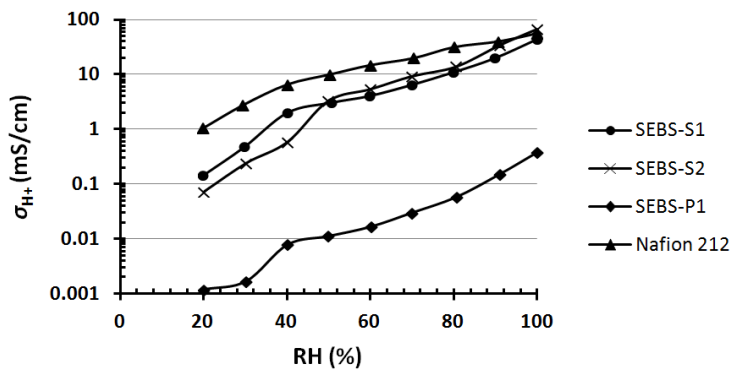


**Figure 3.** Proton conductivity of SEBS-<sub>1a</sub>, SEBS-<sub>2a</sub>, SEBS-P<sub>1a</sub>, and Nafion as a function of relative humidity at 60 °C.

For phosphonic acid-containing polymers, proton conductivity of one or two orders lower is typically observed compared to that with sulfonic acid-containing polymers. Until now, however,

there was no example of proton conductivity data which compares PEMs with the same molar concentration of sulfonic acid and phosphonic acids. As all three ionic SEBS polymers in this report were prepared from the same borylated precursor polymer, they all have the same ion concentration in the side chain, thus allowing direct comparison of sulfonic acid vs. phosphonic acid on PEM side chains. In the case of SEBS-P<sub>1a</sub>, lower acidity of phosphoric acid ( $pK_a = 2$ ) than that of sulfuric acid ( $pK_a = -3$ ) caused the lowest proton conductivity as well as the lowest water uptake in spite of the highest IEC value among all samples.

Hydrophilic and hydrophobic phase separation also affects proton conductivity and surface properties of membrane since inter-connected hydrophilic ionic domains form effective ion conducting pathway. The size and spatial arrangements of microdomains of SEBS and its sulfonated and phosphonated polymers were studied using small angle X-ray scattering (SAXS). Morphology of a block copolymer can be diverse depending on volume ratio of different microdomains, such as spheres in a cubic lattice, cylindrical in the hexagonal packing and lamellar arrangements. To enhance the sensitivity of scattering data signal, the acid groups of SEBS ionomers were exchanged to  $Na^+$  form and their SAXS profiles are compared with that of pristine SEBS in Figure 4. Pristine SEBS displayed three broad scattering peaks at  $q^*$ ,  $\sqrt{3}q^*$ , and  $\sqrt{4}q^*$  suggesting a cylindrical morphology. All acid-functionalized polymer samples also exhibited at least three different scattering peaks: an intense first order peak (represented as  $q^*$ ) and weak second and third order peaks represented as  $2q^*$  and  $3q^*$  respectively. However, after the incorporation of the acid functionalities, the morphology is seem to transform from the cylindrical structure to lamellar structure. For SEBS-S<sub>2Na</sub>,  $2q^*$  value was exactly 2 times higher than  $q^*$  value (i.e.,  $q^* = 0.0121 \text{ \AA}^{-1}$  and  $2q^* = 0.0242 \text{ \AA}^{-1}$ ) and  $3q^*$  was exactly 3 times higher than  $q^*$  (i.e.,  $3q^* = 0.0363 \text{ \AA}^{-1}$ ) which can be attributed to the well-ordered lamellar structure.

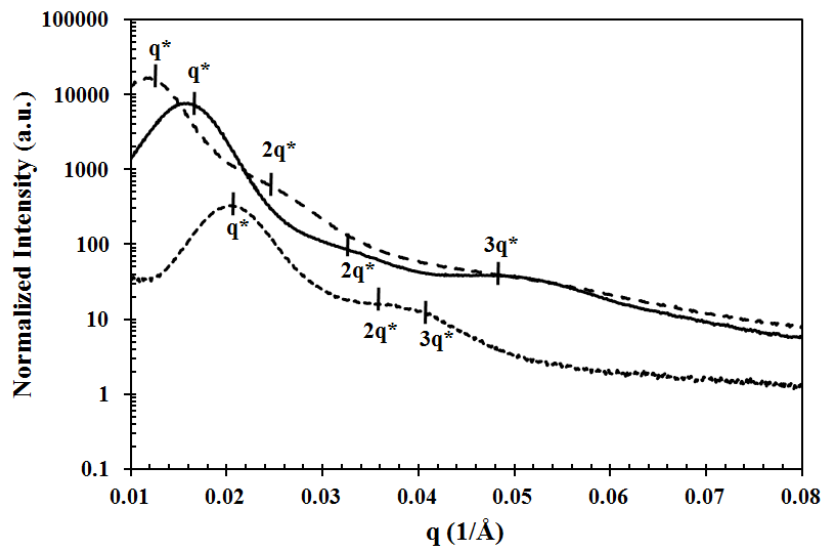


Figure 4. SAXS data of of SEBS-S1, SEBS-S2, and SEBS-P1.

### Versatile Functionalization of Aromatic Polysulfones via Thiol-Ene Click Chemistry

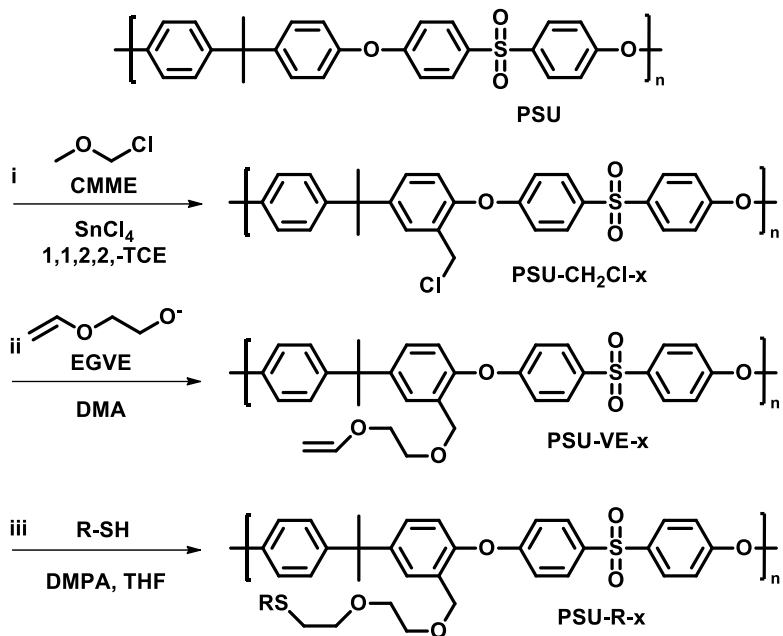
Aromatic polysulfone (PSU) is among the most popular engineering thermoplastics and has been used in a wide range of applications owing to its durable mechanical, physical, and chemical properties. For example, PSU fabricated into membranes has been used in industrial applications such as filtration, fuel cells, gas separation, and biomaterials. Introducing desired

functional groups into the side chains of the polymer backbone creates new functional polymers and broadens the applications of these materials. Over the past decades, several modification strategies have been developed for the preparation of functionalized PSU. These approaches include physical blending or coating and chemical modification. For example, the addition of hydrophilic groups to PSU enhances the inherent hydrophobicity of the material, which improves antifouling properties and extends the life of the polymer membranes in membrane separation applications. Functionalized PSU can also interact specifically with gas molecules for improved selectivity in gas separation processes.

Controlled post-polymerization modification conveniently transforms a common polymer into functional macromolecules without sacrificing its favorable properties, thereby increasing the value of polymer materials. It also incorporates functionalities that cannot be obtained through copolymerization. Because PSU has many desirable properties, its post-polymerization with processes including sulfonation, bromination, lithiation, and haloalkylation has been widely studied. We have reported PSU functionalization via C–H borylation, which incorporates a variety of functional groups under relatively milder reaction conditions. However, the need for expensive transition metal catalysts (i.e., iridium and palladium) has prevented the broad use of this route in a large-scale synthesis.

Click chemistry is a popular post-polymerization modification method owing to its rapid reaction, mild conditions, high yield, and good functional group tolerance. When one half of the functional click chemistry pair is introduced to a polymer chain, it serves as a platform on which to generate various chemical functionalities by efficiently forming covalent bonds with its click counterpart. Among click chemistry reactions, the copper-catalyzed azide-alkyne cycloaddition (CuAAC) reaction has been used most extensively to synthesize functionalized polymers. Once azide-functionalized PSUs are prepared, they can undergo CuAAC with various alkyne derivatives containing different functional groups. Despite the high fidelity of CuAAC-based polymer modifications, the use of potentially hazardous azide compounds makes the click reaction less appealing. Furthermore, polymer materials modified with the CuAAC reaction require extra purification steps to ensure the complete (or nearly complete) removal of toxic heavy metal impurities, especially if the materials are intended for biological applications. For broadened use of functionalized PSUs, metal-free, less hazardous synthetic strategies are highly desirable.

Herein we describe a versatile synthetic approach to aromatic polymer synthesis based on thiol-ene click chemistry. With all the characteristics of click reactions, polymer functionalization with this chemistry provides a number of benefits over other chemical modification methods. First, it uses a harmless metal-free reaction that enables simple workup without the need to remove toxic impurities. Second, the radical reaction can be photo-initiated, which offers improved efficiency and shorter reaction times for complete conversion compared with those of thermally initiated reactions. Third, a wide variety of thiol-terminated molecules are readily available, thus allowing the preparation of diverse polymer derivatives with tunable properties. To demonstrate the versatility of aromatic polymer functionalization with the thiol-ene reaction, we synthesized “clickable” PSU with a pendant double bond as a thiol-reactive precursor polymer that can be further modified with various thiol-containing molecules. Despite the importance of chemical functionality in PSU-based membrane separation technology, to the best of our knowledge, the preparation of functionalized PSU via a thiol-ene click reaction has never been reported.



**Scheme 1.** Synthesis of thiol-ene click-functionalized PSU using a vinyl ether pendant group. Conditions: (i) 50 °C, 50 min; (ii) 5 °C, 30 min; (iii)  $\lambda = 365$  nm, 4 min.

Scheme 1 describes the chemical transformations of PSU performed in this study. PSU was first activated via chloromethylation to set the desired functional degree. The chloromethylated polymer (PSU-CH<sub>2</sub>Cl-x, where x indicates the mol.% of the functional degree in the repeating unit) was subsequently converted to an alkanyl-functionalized polymer (PSU-VE-x) via reaction with vinyl ether containing alkoxide. The vinyl ether group served as a synthetic platform on which to create diverse functional groups in the polymer by using photo-initiated thiol-ene chemistry (PSU-R-x in Scheme 1; see Figure 7 for structures of R). Because the S<sub>N</sub>2 reaction of PSU-CH<sub>2</sub>Cl-x with ethylene glycol vinyl ether and subsequent thiol-ene reactions led to quantitative conversion under mild conditions, the functional degree of the final polymers was easily controlled by adding a targeted concentration of chloromethyl group in the polymer.

Each stage of the sequential transformations of the PSUs was confirmed with <sup>1</sup>H NMR spectroscopy (Figure 5). The conversion of the chloromethyl side group to the terminal alkene was evidenced by the disappearance of the –CH<sub>2</sub>Cl peak (4.54 ppm) and the appearance of a new peak for –CH<sub>2</sub>OCH<sub>2</sub>CH<sub>2</sub> at 4.50 ppm. Additional proton resonances at 6.38, 4.11, and 3.95 ppm with expected integral values and coupling patterns also suggest successful installation of a vinyl ether group to PSU with the expected functionalization degree. We selected benzyl thiol as a model compound for the screening of the click reaction and found that quantitative conversion could be achieved a short time after UVA (365 nm) irradiation with 2,2-dimethoxy-2-phenylacetophenone (DMPA) as an initiator. The peaks assigned to the vinyl ether group disappeared completely, and new peaks appeared that corresponded to the benzyl group formed at the end of the side chain. The relative integral values of benzyl thioether (C<sub>6</sub>H<sub>5</sub>–CH<sub>2</sub>S–; **h** in Figure 5) relative to isopropylidene in the PSU backbone (**5** in Figure 5) matched well with the expected degree of functionalization of the polymer.

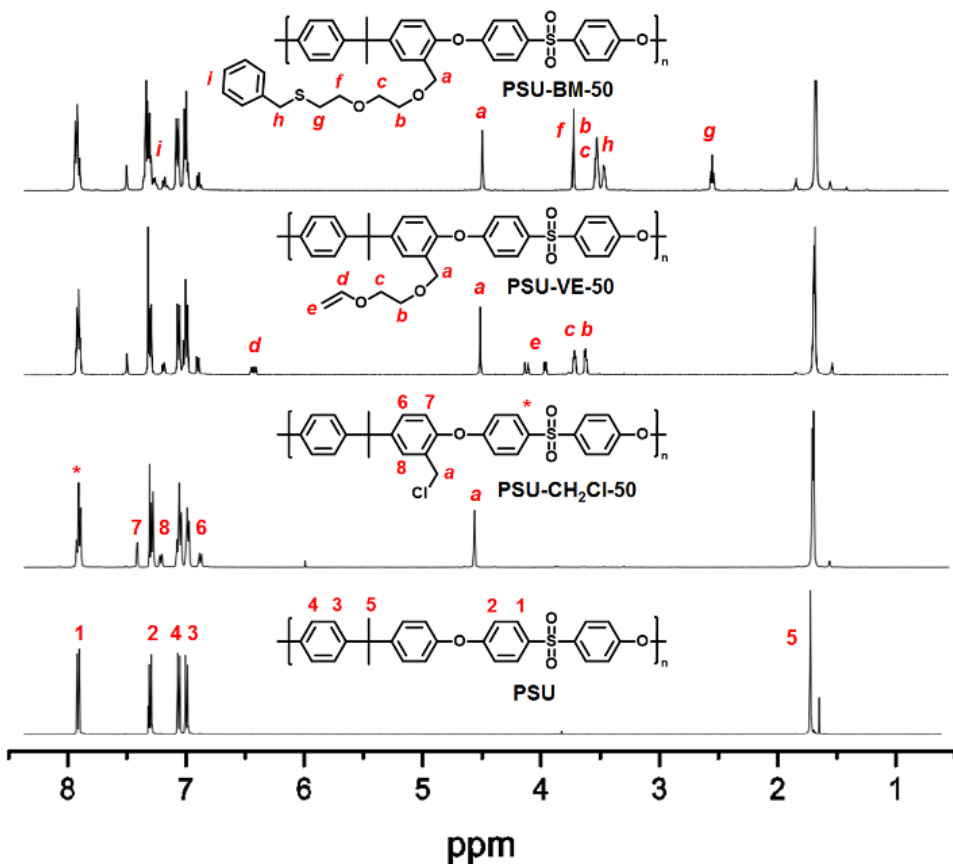


**Figure 5.**  $^1\text{H}$  NMR spectra of PSU, PSU-CH<sub>2</sub>Cl-50, PSU-VE-50, PSU-BM-50.

We introduced an alkenyl moiety to PSU for thiol-ene click polymer reaction because a thiol pendant group in the polymer may undergo oxidation and disulfide formation may occur between polymer chains during storage and subsequent reactions, respectively. In the post-functionalization of commercial polymers, preventing side reactions that change molecular weight significantly via the cleavage or coupling of the polymer chains is critical to maintaining the desired properties of the precursor polymers. The aryl ether bond of the PSU backbone is unstable under highly alkaline conditions; thus, the alkenyl functionalization of PSU-CH<sub>2</sub>Cl-x with the alkoxide nucleophile was conducted in an ice bath. Gel permeation chromatography (GPC) data showed that the vinyl ether functionalized PSU retained the molecular weight properties of the precursor polymer ( $M_n = 37.7$  kg/mol and  $M_w/M_n = 1.9$  for PSU-CH<sub>2</sub>Cl-50;  $M_n = 34.2$  kg/mol and  $M_w/M_n = 1.8$  for PSU-VE-50; see Figure 6 and Table 2). We observed no significant change in these molecular weight properties even after the thiol-ene click reaction with benzyl thiol, which demonstrated the mild nature of this synthetic approach ( $M_n = 37.2$  kg/mol and  $M_w/M_n = 1.9$  for PSU-BM-50). The vinyl ether containing polymer exhibited good solubility in common organic solvents such as chlorinated and polar aprotic solvents, which allowed broader choice of thiol molecules for subsequent click reactions.

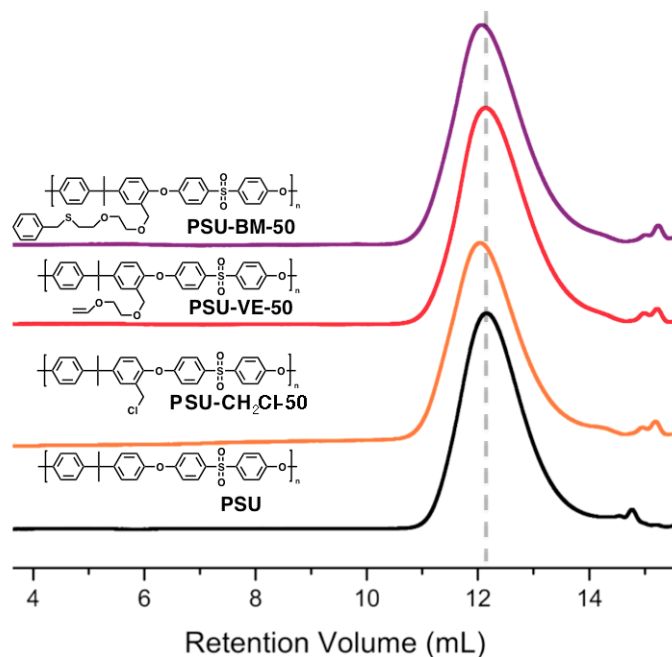


**Figure 6.** GPC traces for PSU, PSU-CH<sub>2</sub>Cl-50, PSU-VE-50, and PSU-BM-50.

**Table 2.** Molecular weight properties of functionalized PSUs.

Polymer	DF (%) <sup>a</sup>	$M_n$ <sup>b</sup>	$M_w$ <sup>b</sup>	$M_w/M_n$ <sup>b</sup>
<b>PSU</b>	0	32.8	61.5	1.9
<b>PSU-CH<sub>2</sub>Cl-50</b>	50	37.7	73.5	1.9
<b>PSU-VE-50</b>	50	34.2	63.1	1.8
<b>PSU-BM-50</b>	50	37.2	71.0	1.9
<b>PSU-HT-50</b>	50	57.6	132.0	2.3
<b>PSU-MPP-50</b>	50	49.4	105.0	2.1
<b>PSU-ME-50</b>	50	36.9	94.4	2.6
<b>PSU-TEG-50</b>	50	50.5	114.0	2.3
<b>PSU-TGG-50</b>	50	51.3	90.0	1.8

<sup>a</sup>Degree of functionalization determined with <sup>1</sup>H NMR analysis.

<sup>b</sup>Determined with GPC in THF using polystyrene standards (kg/mol).

Functionalized PSUs have gained significant interest owing to the diversity of their potential applications, which include membrane-based gas separation, water purification, biomedical devices, and fuel cells. To test the versatility of thiol-ene chemistry in the post-functionalization of PSU, we reacted six commercial thiols having various chemical functionalities with a vinyl ether containing precursor polymer. These thiol substrates contained an aromatic ring (BM), an alkyl chain (HT), an ester (MPP), an alcohol (ME), an ethylene glycol ether (TEG), and a glucose ester molecule (TGT; Figure 7). Full characterization of the resulting thiol-ene functionalized polymers was carried out with <sup>1</sup>H NMR and FTIR. Due to the high reactivity of the vinyl ether group in the thiol-ene reaction, most of the thiols in Figure 7 required short irradiation times (typically less than 5 min) to achieve full conversion. One exception was TEG, which took a longer time (30 min) for full conversion, likely owing to its longer chain length and

steric shielding effect on the terminal thiol moiety. GPC analysis of molecular weights after the thiol-ene click reactions showed a minor increase in molecular weight, which is attributed to the increased hydrodynamic volume of the polymer after the attachment of functional groups to the side chain (Table 2).

For efficient post-polymerization modifications, a polymer substrate must have a precursor group that is stable during storage but highly reactive on activation. To study the reactivity of alkenyl structures toward the click reaction, we investigated two types of C=C bond structures attached to PSU: vinyl ether and allyl ether. The allyl ether functionalized polymer—PSU-AE-50—was prepared by reacting PSU-VE-50 with allyl alcohol instead of ethylene glycol vinyl ether. Both vinyl ether and allyl ether quantitatively react with thiols, but compared with other types of alkenyl structures, a vinyl ether group, which has more electron-rich C=C bonds, is expected to be more reactive in thiol-ene click reactions. Methyl 3-mercaptopropionate (MPP in Figure 7) was used as the thiol to compare the reactivity toward two different C=C bond structures. After fewer than 5 min of UV irradiation, the C=C bond of the vinyl ether in PSU-VE-50 was fully converted to a thioether bond to yield PSU-MPP-50. Under the same conditions, the C=C bond of the allyl ether group was less reactive and required a slightly longer irradiation time for complete conversion (60% in 5 min and >99% in 7 min).

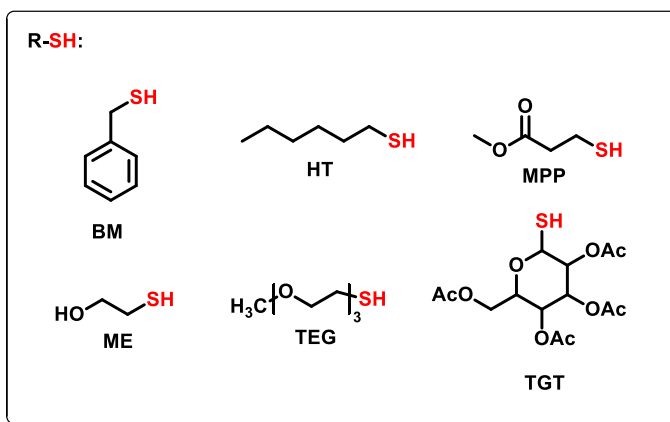


**Figure 7.** Thiol small molecules with various functional groups used for thiol-ene click reactions with PSU.

The functionalization of the PSU side chain via thiol-ene click chemistry affected the surface properties of the polymer. Synthetic glycopolymers with pendant carbohydrate moieties have been recognized as useful biomaterials owing to their biological activity and specific interactions with aqueous boron species. Because PSU is an excellent polymer material for membrane-based separation applications, attaching glucose molecules via metal-free harmless click chemistry will generate attractive membrane materials for water purification and biomedical uses. Such a glyco-functionalized polymer was successfully prepared through the thiol-ene reaction of PSU-VE-50 with TGT and subsequent removal of the acetate group. The deprotection step was performed in PSU-TGT thin film because the resulting polymer (PSU-G) had poor solubility in organic solvents. The C=O stretching band of PSU-TGT at  $1750\text{ cm}^{-1}$  disappeared, and a new band for O–H stretching at  $3400\text{ cm}^{-1}$  appeared in the PSU-G FTIR spectrum. An increase in the degree of functionalization of PSU-G from 50% to 100% also showed a more intense O–H stretching band.

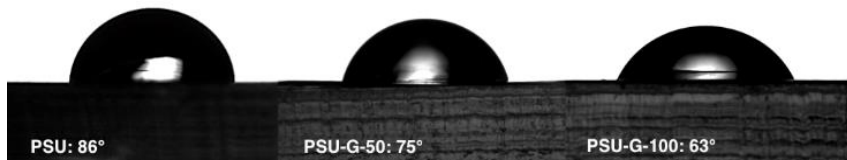


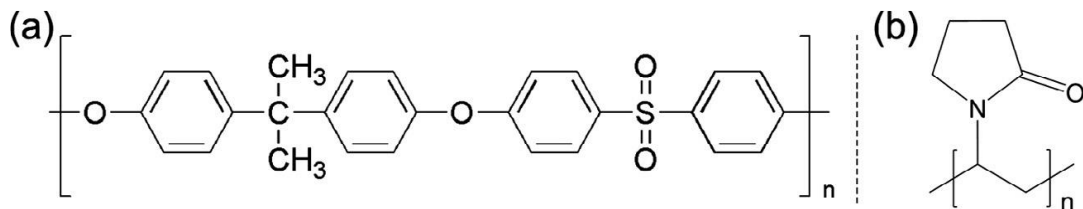
**Figure 8.** Contact angle measurement images of PSU, PSU-G-50, and PSU-G-100.

Despite the excellent stability of pristine PSU membranes, they are inherently hydrophobic, which causes membrane fouling from non-specific adsorption of foulants during filtration processes and is a major drawback. Thus, the preparation of PSU with a more hydrophilic surface is a major research topic in membrane science. The post-functionalizing of PSU with thiol-ene click chemistry offers a convenient and versatile approach to the creation of hydrophilic moieties on the PSU surface and broadens the potential applications of the polymer. To illustrate the effect of functional groups on surface properties of these polymeric materials, we measured the water contact angles of pristine PSU and click-functionalized PSUs. The most drastic change in hydrophilicity was observed for PSU-G, which has a pendant carbohydrate bearing multiple hydroxyl groups; the static contact angle decreased from 86° to 75° when 50% of the repeating unit of PSU was functionalized with glucose. This angle decreased further to 63° when the degree of functionalization was increased to 100% (Figure 8).

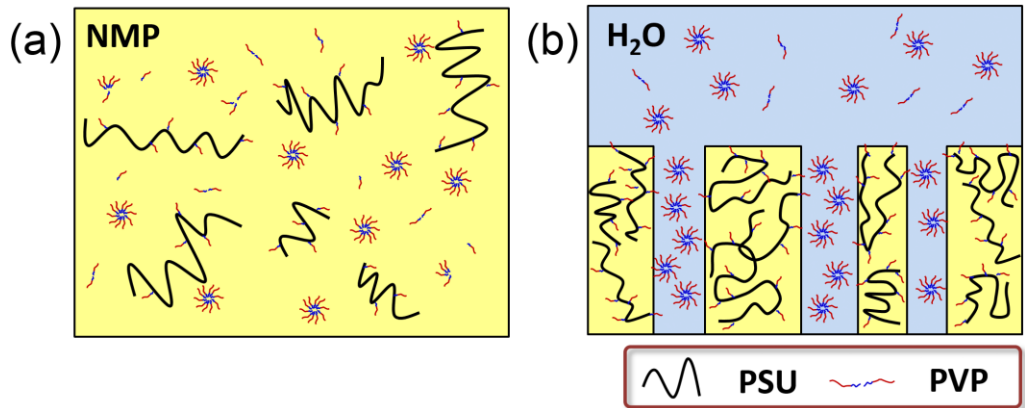
Due to its high efficiency and synthetic versatility, post-polymerization modification strategies using click chemistry have been extensively explored to synthesize functional polymers with tunable properties. This report describes for the first time a convenient chemical functionalization of PSU—a widely used aromatic polymer for membrane applications—that uses thiol-ene click chemistry. Vinyl ether moiety was introduced to the side chain of PSU in controlled concentrations and subsequently converted into various functional groups without causing side reactions or degrading the polymer. The properties of PSU can be tuned for desired purposes by using a pendant vinyl group as a highly reactive precursor and appropriate thiol derivatives. The convenient synthetic strategy in this study yields functionalized aromatic polymers through a process that is simply initiated by a short period of UV irradiation under mild conditions that require neither metal catalysts nor expensive reagents.

### Characterization of PSU/Graphene oxide (GO) membranes

Figure 9 shows the chemical structures of PSU (a) and polyvinylpyrrolidone (PVP) (b). PSU membranes were prepared by the phase inversion method as shown in Figure 10<sup>1,2</sup>. PSU was the membrane matrix, and PVP was the membrane modifier as well as the pore-generating agent. PSU was dissolved in NMP and stirred at 60 °C for 4 hours. At that point, various amounts of PVP were added and the PSU solution was stirred at 60 °C for an additional 4 hours. In order to eliminate bubbles in the solution, a vacuum was applied for 30 min. The solutions were cast on glass plates with a casting knife, and then immersed in a coagulation bath of DI water. In order to reduce error during phase inversion process, the volume and temperature of water bath were equalized. Subsequently, the pristine membranes were peeled off, and were washed thoroughly with DI water to remove residual solvent. These prepared membranes (a wet thickness of approximately 150 µm) were kept in DI water until used.

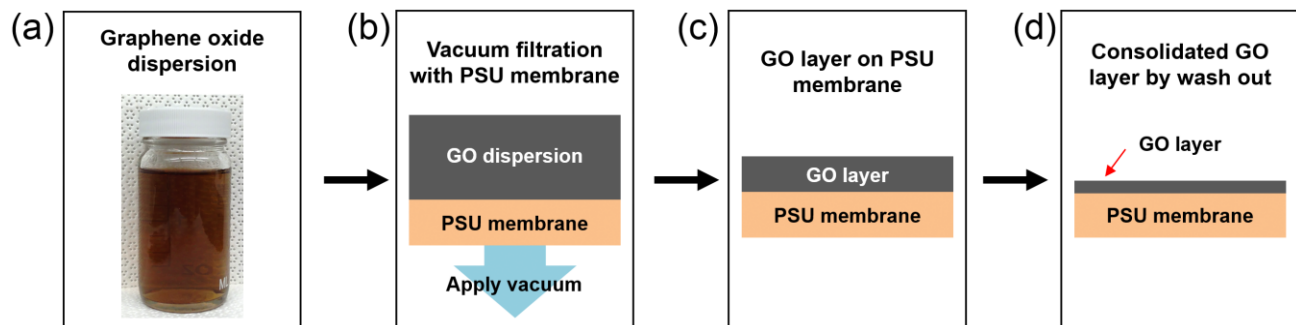


**Figure 9.** Chemical structures of (a) polysulfone and (b) polyvinylpyrrolidone.



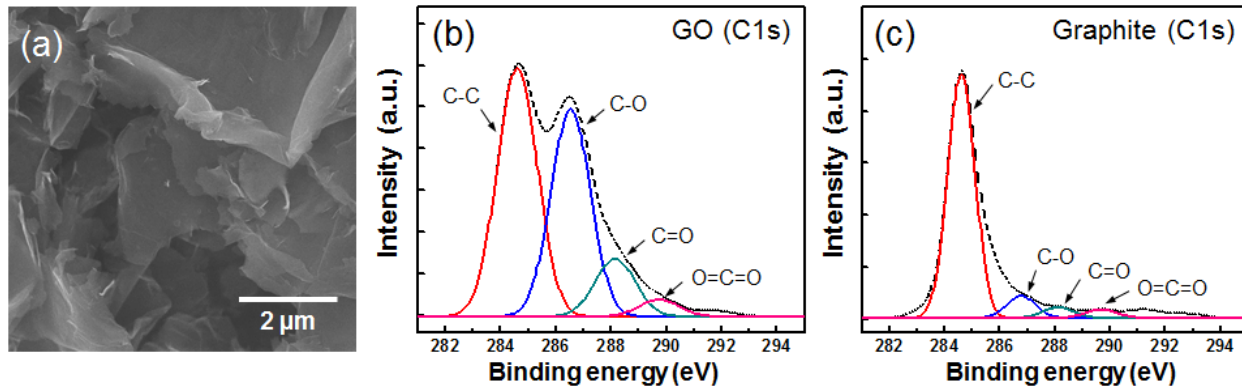
**Figure 10.** The membrane formation process. (a) The PSU polymer and PVP were dispersed homogeneously in NMP and (b) the film was immersed in a DI water bath. This led to phase separation and the formation of ordered structure and pores in membrane by means of phase inversion.

Figure 11 shows that preparation of the PSU/GO membrane. This was carried out by vacuum filtration of the GO dispersion (2 mL) by using the as-prepared PSU membrane (10 wt.% of PVP). After this, extra GO was washed out with DI water to consolidate the layer of GO by eliminating weakly deposited GO.



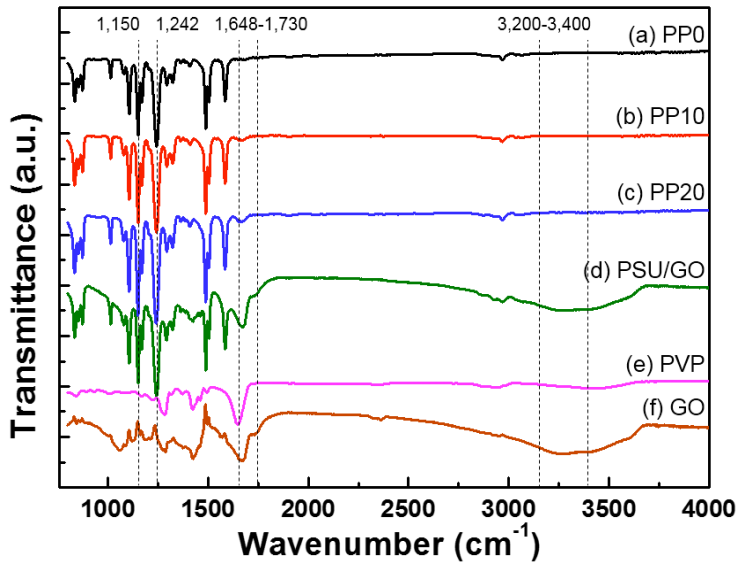
**Figure 11.** Preparation of the PSU/GO membrane. First, (a) GO was dispersed in DI water. (b) Next, vacuum filtration of the GO dispersion took place throughout the PSU membrane and (c) the GO layer formed on the PSU membrane. Finally, (d) extra GO was washed out with DI water to consolidate the layer of GO.

Figure 12a shows the SEM image of the GO sheets, where the folded and wrinkled features of the two-dimensional thin GO sheets had a width of more than several micrometers. Figure 12b and 12c compare the C1s narrow scans of the GO sheets and graphite from the XPS analysis. The spectra of the GO (Figure 12b) consisted of two prominent components that arose due to the C-C bonds at  $\sim$ 284.6 eV and to the C-O (hydroxyl and epoxy) bonds at  $\sim$ 286.5 eV as well as other minor components that result from various oxygenated carbon atoms, such as C=O and O=C=O at  $\sim$ 288.1 and  $\sim$ 289.6 eV, respectively<sup>3</sup>. Before the oxidization process (graphite), the intensity of the C-O component was significantly lower than that of the GO (Figure 12c). The XPS analysis indicated that the prepared GO had a hydrophilic character because of the high oxidization with hydrophilic functional groups.



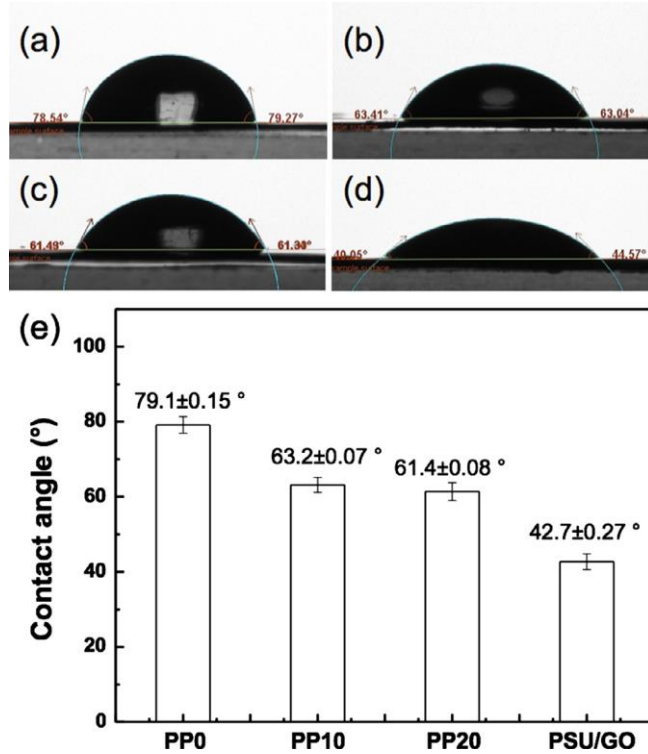
**Figure 12.** The morphology of (a) prepared GO, C1s XPS spectrum of (b) GO, and (c) graphite.

Figure 13 shows the FT-IR spectra of the fabricated membranes (PP0, PP10, PP20, and PSU/GO), PVP as an additive, and GO as a hydrophilic modifier. Figure 13a shows the FT-IR spectrum of the pristine PSU membrane (PP0). Figures 13b and 13c show PVP-blended PSU membranes at 10 and 20 wt.% PVP, respectively. The strong peaks at  $1,150$  and  $1,242\text{ cm}^{-1}$  for PSU and PVP-blended membranes are associated with the stretching vibration of the S=O and C-O-C bond of the PSU, respectively [Figures 13(a-c)]<sup>4</sup>. The peak at  $1,648\text{ cm}^{-1}$  is attributed to the amide carbonyl stretching of PVP, as shown in the Figure 13e. In addition, this peak appears slightly in the spectra obtained from the PVP-blended membranes, as shown in Figures 13b and 13c. Figure 13f shows the spectrum of GO, which has peaks at  $1,730$  and  $3,200\text{-}3,400\text{ cm}^{-1}$  that correspond to the C-O and -OH stretching, respectively. These findings indicate the existence of the hydrophilic functional groups in the GO. The spectrum of the PSU/GO membrane clearly shows a broad band at  $3,200\text{-}3,400\text{ cm}^{-1}$  (Figure 13d), which suggests that the hydrophilic layer formed on the surface of the membrane due to hydrophilic functional groups of the GO.



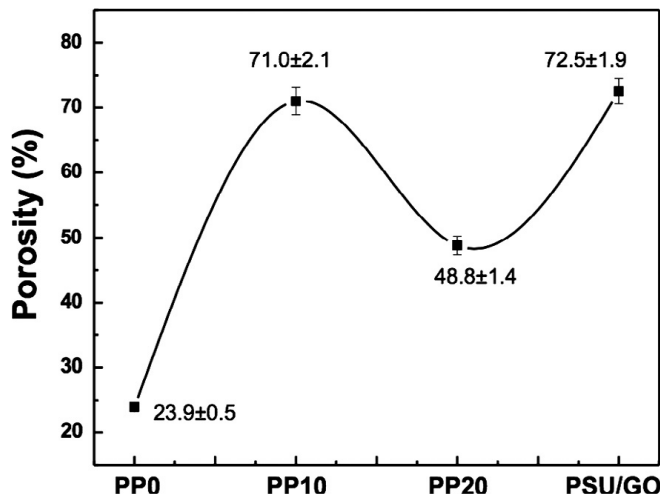
**Figure 13.** FT-IR spectra of (a) PP0, (b) PP10, (c) PP20, (d) PSU/GO membranes, (e) PVP, and (f) GO.

Figures 14a–d shows the water contact angles of PP0, PP10, PP20, and PSU/GO membranes. Surface hydrophilicity is an important factor in determining the antifouling property of the ultrafiltration membranes. The lower contact angle represents the hydrophilic nature to wet the membrane easily, higher surface energy, and higher hydrophilicity. Among all the membranes were tested, the pristine PSU membrane (Figure 14a) shows the higher hydrophobic character with a higher contact angle of about  $79.12^\circ$  than others. The water contact angle decreased as the amount of PVP increased, since hydrophilic functional groups were introduced to the surface of the hydrophobic PSU membrane. Figure 14b and c shows that the addition 10 and 20 wt.% of PVP in the PSU solution decreased the water contact angle of the membranes to  $63.15^\circ$  and  $61.39^\circ$ , respectively. When a layer of the hydrophilic GO was applied on the membrane surface, the water contact angle was further decreased to  $42.72^\circ$  (Figure 14d). Thus, a deposited layer of GO on the PSU membrane maximized the hydrophilic character of the prepared membrane by associating the hydrophilic functional group of the GO sheets, as seen from the XPS and FT-IR results. Figure 14e summarizes the results of the contact angles of the prepared membranes.



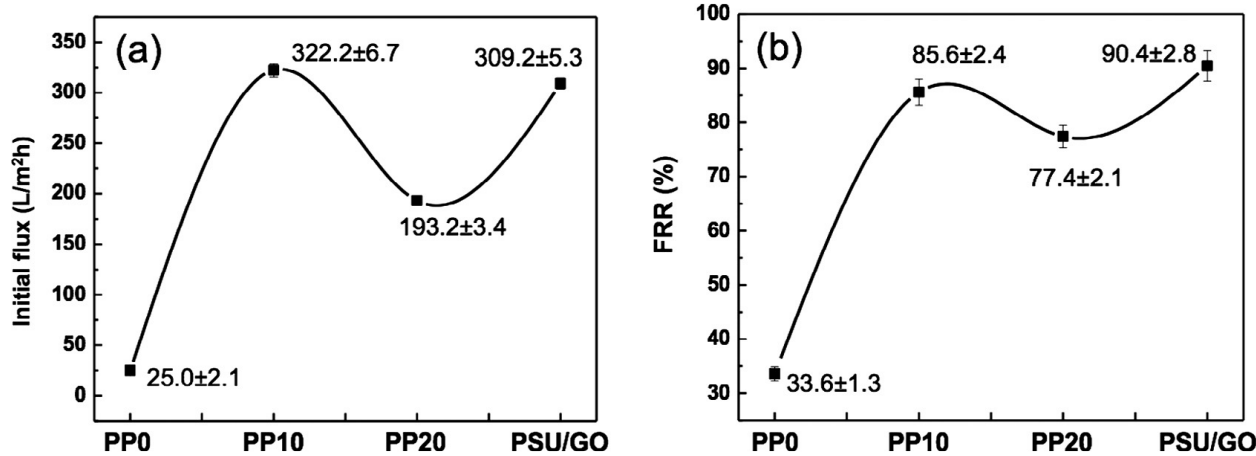
**Figure 14.** Contact angles of the membranes by DI water (a) PP0, (b) PP10, (c) PP20, (d) and PSU/GO; at bottom, (e) summarized results.

Figure 15 presents the porosity of PP0, PP10, PP20, and PSU/GO membranes. The prepared membranes (PP0, PP10, PP20, and PSU/GO) had 23.9%, 71.0%, 48.8%, and 72.5% of porosity, respectively. The hydrophilicity effect of PVP could increase the solvent and non-solvent exchange during the phase-inversion process. On the other hand, when 20 wt.% of PVP was added to the casting solution, the viscosity might be increased. This causes a slow exchange rate between the solvent and nonsolvent and resulting in a lower porosity.



**Figure 15.** Porosity of the prepared PSU membranes (PP0, 10, 20, and PSU/GO).

As shown in Figure 16a and b, the initial water flux and the water FRR (after renewal of the membrane surfaces by washing with DI water) were analyzed to verify the improved antifouling performance by the addition of PVP and the hydrophilic layer of GO. Figure 16a shows the initial results of the pure water flux of the prepared membranes. The pure water flux through membranes shows the non-linear relationship with the PVP contents. The pristine PSU (PP0) had the lowest initial water flux of  $25.0 \text{ L}/(\text{m}^2 \cdot \text{h})$ , and the prepared PP10 membrane had the highest flux of  $322.2 \text{ L}/(\text{m}^2 \cdot \text{h})$ . However, a higher additive concentration (PP20) in the membranes led to a decrease in flux [ $193.2 \text{ L}/(\text{m}^2 \cdot \text{h})$ ]. When added high concentration of PVP in cast solution, the reduction of pure water flux would be correlated with delayed polymer coagulation on the surface region during phase inversion process. Therefore, lowering the pure water flux data with 20 wt.% content of PVP may suggest that the balance in correlation between enhancement of thermodynamic and inhibition of rheological diffusion. The layer of GO-added membrane had  $309.2 \text{ L}/(\text{m}^2 \cdot \text{h})$  of initial water flux, which was slightly lower than for PP10. Although PSU/GO was fabricated from PP10, one additional thin layer of GO reduced the initial water flux. The FRRs of the prepared membranes are depicted in Figure 16b. A higher FRR indicates better antifouling performance of the membrane. The FRR for the pristine PSU membrane (33.6%) was lower than the FRR for the membranes prepared by adding PVP or GO (more than 75.0%). It is proposed that some protein molecules may deposit on the membrane surface or clog the membrane pore. PP10, PP20, and PSU/GO had FRRs of 85.6%, 77.4%, and 90.4%, respectively. Although PSU/GO membranes showed a lower initial flux than PP10, the higher hydrophilicity of the PSU/GO membrane decreased the interactions between bio-contaminants and the membrane surface, leading to decreased contaminant adsorptions or being able to remove the fouling layers more easily<sup>5,6</sup>. Additionally, these experimental results indicated that the antifouling performance of the PSU/GO ultrafiltration membrane was improved by the hydrophilic nature of the GO layer.



**Figure 16.** Initial flux (a) and FRR results (b) of the fabricated PSU membranes (PP0, 10, 20, and PSU/GO).

**3. Comparison of actual accomplishment and explanation of variance**

No variation from the planned activities.

**4. Plans for next report period**

This is a final report

**5. Cost status**

DOE funds are 100% expended.

**6. Schedule status**

N/A

**7. Changes in approach or aims and reasons**

None.

**8. Actual or anticipated problems or delays**

N/A

**9. Changes of key personnel**

None

**10. Product produced or technology transfer activities**

T. Hwang, J.-S. Oh, W. Yim, J.-D. Nam, C. Bae, H.-I. Kim, and K. J. Kim, Ultrafiltration using graphene oxide surface-embedded polysulfone membranes, *Separation and Purification Technology* 166 (2016) 41-47.

**11. References**

- [1] S.P. Roux, E.P. Jacobs, A.J.V. Reenen, C. Morkel and M. Meincken, Hydrophilisation of polysulphone ultrafiltration membranes by incorporation of branched PEO-block-PSU copolymers, *Journal of Membrane Science* 276 (2006) 8-15.
- [2] R. Lv, J. Zhou, Q. Du, H. Wang and W. Zhong, Preparation and characterization of EVOH/PVP membranes via thermally induced phase separation, *Journal of Membrane Science* 281 (2006) 700-706.
- [3] H.-J. Shin, K.K. Kim, A. Benayad, S.-M. Yoon, H.K. Park, I.-S. Jung, M.H. Jin, H.-K. Jeong, J.M. Kim, J.-Y. Choi and Y.H. Lee, Efficient reduction of graphite oxide by sodium borohydride and its effect on electrical conductance, *Advanced Functional Materials* 19 (2009) 1987-1992.
- [4] R. Kumar, A.M. Islloor, A.F. Ismail, S.A. Rashid and T. Matsuura, Polysulfone-Chitosan blend ultrafiltration membranes: preparation, characterization, permeation and antifouling properties, *RSC Advances* 3 (2013) 7855-7861.
- [5] K.A. Mahmoud, B. Mansoor, A. Mansour, and M. Khraisheh, Functional graphene nanosheets: the next generation membranes for water desalination, *Desalination* 356 (2015) 208–225.

[6] J. Lee, H.-R. Chae, Y.J. Won, K. Lee, C.-H. Lee, H.H. Lee, I.-C. Kim, and J.-M. Lee, Graphene oxide nanoplatelets composite membrane with hydrophilic and antifouling properties for wastewater treatment, *Journal of Membrane Science* 448 (2013) 223–230.